Hybrid memory layer with low Curie temperature CoPd/Pd multilayer for high-density magnetic random-access memory cells

W. Zhao[1], X. Dong[1], T. Kimura[1], T. Kato[1], D. Oshima[2], Y. Sonobe[3], Y. Kawato[3], S. Iwata[2]

[1]Department of Electronics, Nagoya University, Nagoya, Aichi 464-8603, Japan
[2]Institute of Materials and Systems for Sustainability, Nagoya University, Nagoya, Aichi 464-8603, Japan
[3]Samsung R&D Institute Japan, Yokohama, Kanagawa 230-0027, Japan

We investigated switching behavior of the hybrid structures consisting of low Curie temperature (T_C) and high T_C layers. The T_C of [Co (0.3 nm) / Pd (1.2 nm)]$_6$ and [$Co_{54}Pd_{46}$ (0.3 nm) / Pd (1.2 nm)]$_6$ multilayers (MLs) were confirmed to have much higher than 200˚C and around 110˚C, respectively. In the bi-MLs hybrid structure with Co / Pd and CoPd / Pd MLs, the two MLs are exchange coupled at room temperature, and the CoPd / Pd ML was switched following the magnetization of the high T_C Co / Pd ML at high temperature (~170˚C) at which the CoPd / Pd ML becomes paramagnetic. The tri-layered hybrid structure with a stack of [Co (0.4 nm) / Pt (1.2 nm)]$_6$ / [$Co_{48}Pd_{52}$ (0.3 nm) / Pd (1.2 nm)]$_3$ / [Co (0.4 nm) / Pd (1.2 nm)]$_3$ was also investigated. The tri-MLs stack showed one-step hysteresis loop at room temperature and two-steps loop at higher than 120˚C due to the loss of magnetic order of the intermediate low T_C CoPd / Pd ML. From the data of tri-MLs stack, the exchange coupled and decoupled situations between Co / Pt and Co / Pd MLs were found to be realized by changing the temperature from room temperature to around 150˚C.

***Index Terms*— Co based multilayer, Curie temperature, exchange coupling, MRAM**

I. Introduction

Spin transfer torque (STT) switching is considered a promising writing procedure to realize Gbit-class magnetic random access memory (MRAM) [1], [2]. For the development of high-density MRAM comparable to working memory, both a low critical current I_c of STT switching for the writing process and a high thermal stability factor (Δ) for nonvolatile memory operation are required [3]. However, since the STT critical current I_c is proportional to the Δ, it is necessary to find a better compromise between I_c and Δ to realize the high-density MRAM. One solution to reduce the critical current I_c without this compromise is thermally assisted switching MRAM [4], [5]. In this switching scheme, heating of the MRAM cell during the writing reduces the critical current I_c, since the I_c scales with the energy barrier of the magnetization reversal and the barrier height reduces with elevating temperature. We have previously studied STT switching of GdFeCo single and GdFeCo / TbFe bilayers to study the effect of heating on the relationship between the critical current density J_c and Δ [6]–[9], since the amorphous rare earth (RE) transition metal (TM) alloys are known to exhibit large perpendicular anisotropy and their Curie temperatures were easily tuned by varying the composition of the alloy [10]–[14]. In the previous studies we reported the significant gain on the ratio of Δ / J_c by employing the bilayer GdFeCo / TbFe compared the single GdFeCo layer. Recently, a novel Curie temperature (T_C) composite hybrid memory structure (T_CC structure) has been proposed to reduce the switching current I_c maintaining sufficient Δ. The T_CC structure is supposed as a double-layered hybrid stack with high T_C and low Δ exchange-coupled to another layer with low T_C and high Δ, and significant gain (~4) of the ratio Δ / I_c compared to the conventional STT switching is expected [15] . This T_CC scheme also reported for the improvement of the performance in the heat assisted magnetic recording [16].

The Co / Pd and Co / Pt multilayers (MLs) with a perpendicular magnetic anisotropy have been first reported for magneto-optical recording media [17], [18]. The T_C of the Co / Pt ML can be lowered by decreasing the Co layer thickness and increasing the Pt layer thickness, but it is generally difficult to make T_C lower than 300°C [19]. To fulfill the requirement of low T_C, for the TcC structure, we propose to use CoPd / Pd ML, since the T_C of CoPd alloy can be lowered by increasing Pd concentration [20]. Furthermore, CoPd / Pd ML show a sufficiently large perpendicular anisotropy for the low T_C layer of the T_CC structure [21].

We report the temperature dependence of coercivity and Kerr rotation of Co / Pd ML, CoPd alloy and CoPd / Pd ML to show the CoPd / Pd ML is useful for the low T_C layer of the T_CC structure. Then we fabricated the bi-layered hybrid stack with high T_C ML exchange-coupled to low T_C ML, and studied the magnetization switching of the hybrid stack. Finally, we report tri-layered hybrid stack with two high T_C MLs intermediated by a low T_C ML, since the tri-layered stack is expected to be more efficient than bi-layered stack.

II. Experimental method

CoPd alloy, Co / Pd (Pt) MLs, CoPd / Pd MLs, and their hybrid stacks were fabricated by magnetron sputtering on thermally oxidized silicon substrates. The CoPd alloy layers were fabricated by co-sputtering of Co and Pd, and the alloy composition was controlled by adjusting the sputtering powers applied to the two targets. All the layers were deposited at room temperature. Hysteresis loops were measured by alternating gradient field magnetometer (AGM). The Curie temperature T_C was estimated by measuring the Kerr rotation at different sample temperatures. The polar Kerr rotation was measured by a polarized angle modulation method.

III. RESULTS AND DISCUSSIONS

A. *Magnetic properties of CoPd / Pd ML*

In the T_CC hybrid stacks, the Co / Pd ML was supposed to act as the high T_C layer. We fabricated a stack of substrate / Ta (10 nm) / Pd (5 nm) / [Pd (1.2 nm) / Co (0.3 nm)]$_6$ ML / Ta (2 nm) and the hysteresis loop of the ML was measured at the room temperature as shown in Fig. 1 (a). Blue and red lines show the loops taken applying the external field perpendicular and parallel to the film plane, respectively. The Co / Pd ML shows a squareness about 1 in the perpendicular loop. The temperature dependence of Kerr rotation and perpendicular coercivity of the Co / Pd ML is shown in Fig.1 (c) as green triangles. With increasing temperature, the Kerr rotation and coercivity descended gradually, and the T_C of Co / Pd ML is expected to be over 200°C, which is appropriate for the high T_C layer in the T_CC structure.

FIGURE 1 HERE

To find a structure having low T_C, we fabricated CoPd (20 nm) single layers as a stack of substrate / Ta (10 nm) / $Co_{54}Pd_{46}$ (20 nm) / Ta (2 nm). Red circles in Fig. 1 (c) show the temperature dependence of Kerr rotation of $Co_{54}Pd_{46}$ (20 nm). (The alloy film exhibited in-plane easy axis, and the data of the perpendicular coercivity were not shown in the figure.) The Kerr rotation was almost constant up to 200°C, indicating that the T_C of the $Co_{54}Pd_{46}$ (20 nm) alloy is much higher than 200°C.

Then we fabricated [$Co_{54}Pd_{46}$ (0.3 nm) / Pd (1.2 nm)]$_6$ ML with a stack of substrate / Ta (10 nm) / Pd (5 nm) / ML / Ta (2 nm) to verify its Curie temperature. The polar Kerr loops, taken at different temperatures and applying an external field along perpendicular to the plane, are shown in Fig. 1 (b), and the temperature dependence of Kerr rotation and perpendicular coercivity of the CoPd / Pd ML is shown in Fig. 1 (c) as blue diamonds.

According to the Kerr loop, the CoPd / Pd ML showed a large perpendicular anisotropy, and the squareness of the ML was almost 1 at room temperature. With increasing temperature, the coercivity became 0 Oe over 86°C, and the squareness significantly reduced above 86˚C due to the reduction of perpendicular anisotropy. The Kerr rotation became 0˚ over 110°C, indicating the T_C of the CoPd / Pd ML significantly decreased to 110°C unlike the CoPd (20 nm) single layer, and thus the CoPd / Pd ML can be used as low T_C layer in the T_CC hybrid stack.

B. *Bi-layer structure*

We have shown the Co / Pd MLs have T_C over 200°C, and CoPd / Pd MLs have T_C as low as 110°C. To study the magnetic properties of the T_CC hybrid stack, we fabricated high T_C Co / Pd ML exchange coupled to low T_C CoPd / Pd ML. The intensity of exchange coupling was controlled by inserting Pd (t_{Pd}) layer with thicknesses of t_{Pd} = 0 – 5 nm.

FIGURE 2 HERE

Figure 2 (a) shows polar Kerr loops of [CoPd (0.3 nm) / Pd (1.2 nm)]$_6$ / Pd (t_{Pd}) / [Co (0.3 nm) / Pd (1.2 nm)]$_6$ exchange coupled stacks with t_{Pd} = 0 nm (upper) and 5 nm (lower). From Fig. 2 (a), both stacks were confirmed to have perpendicular easy axis. For t_{Pd} = 0 nm, the stack exhibited one-step loop, meaning high T_C Co / Pd ML exchange-coupled to low T_C CoPd / Pd ML, and simultaneous switching of both layer took place at a coercive field. On the other hand, for t_{Pd} = 5 nm, the stack exhibited two-steps loop, meaning two layers switched independently due to the small exchange coupling between the two layers. As shown by green triangles in Fig. 2 (b), the Kerr rotation and coercivity of the hybrid stack with t_{Pd} = 0 nm decreased gradually with increasing temperature. For the hybrid stack with t_{Pd} = 5 nm, lower and higher coercivities, referred to as H_{cL} and H_{cH}, respectively, are estimated, and the temperature dependence of the two coercivities and Kerr rotation is shown in Fig. 2 (b). The H_{cL} (blue squares) was gradually decreased up to 50˚C and greatly decreased to 0 Oe from 50˚C to 90˚C, whereas the H_{cH} (red circles) drastically decreased up to 50˚C then gradually decreased. From this temperature dependence, lower (higher) coercivity at room temperature is due to the switching of Co / Pd (CoPd / Pd) ML, however, at the temperature > 50˚C, the lower (higher) coercivity is due to the switching of CoPd / Pd (Co / Pd) ML. Moreover, the coercivity of the exchange coupled stack (t_{Pd} = 0 nm) is considered to be dominated by the H_c of the Co / Pd ML. The Kerr rotation of the stack with t_{Pd} = 5 nm (red diamonds) decreased significantly up to 110˚C due to the reduction of the magnetization of low T_C CoPd / Pd, and became almost constant at temperature > 110˚C.

The magnetization switching behavior of the T_CC hybrid structure consisting of Co / Pd and CoPd / Pd MLs was confirmed by applying external fields during the heat cycle. Figures 3 (a) and (b) show the switching behaviors of [CoPd (0.3 nm) / Pd (1.2 nm)]$_6$ / Pd (t_{Pd}) / [Co (0.3 nm) / Pd (1.2 nm)]$_6$ hybrid stacks with t_{Pd} = (a) 0 nm and (b) 5 nm, respectively. The solid and open symbols are the results of the 1st and 2nd heat cycles, respectively.

FIGURE 3 HERE

At first, we applied an external field H_{ext} = +7 kOe to saturate the stacks to upward (upward is defined as plus direction in Fig. 3). Then we increased temperature under a small positive field of H_{ext} = 20-60 Oe, which is a residual field of the electromagnet. As shown in the red symbols in the Figs (a) and (b), the Kerr rotation of both films decreased. The Kerr rotation became almost constant at temperature > 140˚C for the stack t_{Pd} = 0 nm and > 110˚C for the stack t_{Pd} = 5 nm. These phenomena are understood by the loss of the magnetic order of the low T_C CoPd / Pd ML. Next, at around 170°C, the external field H_{ext} = –2 kOe was applied to switch the magnetization of the stacks to downward. In the 1st cycle small negative field H_{ext} = –40 Oe was applied during the cooling down (blue closed circles), whereas positive H_{ext} = +40 Oe was applied for the 2nd cycle (blue open circles). As shown in Fig. 3 (a), the stack with t_{Pd} = 0 nm showed a similar trend between the 1st and 2nd cycles, i.e., the Kerr rotation decreased with decreasing the temperature for both cycles. This indicates that the magnetization of the low T_C CoPd / Pd ML aligned downward for both cycles, and the switching of low T_C CoPd / Pd was controlled by the magnetization direction of the high T_C Co / Pd ML through the exchange coupling between the two MLs. On the other hand, the stack with t_{Pd} = 5 nm showed different temperature dependence between the 1st and 2nd cycles. When the positive field H_{ext} = +40 Oe was applied, the Kerr rotation increased with decreasing the temperature, whereas, when H_{ext} = –40 Oe, the Kerr rotation decreased. The difference is originated from the difference of the direction of the low T_C CoPd / Pd layer, and thus the switching of low T_C CoPd / Pd was determined by H_{ext} during the cooling for the stack with t_{Pd} = 5 nm.

Figure 4 (a) shows Pd thickness dependence of Curie temperature of the low T_C ML in [CoPd (0.3 nm) / Pd (1.2 nm)]$_6$ / Pd (t_{Pd}) / [Co (0.3 nm) / Pd (1.2 nm)]$_6$ hybrid stack. The Curie temperature was estimated from the temperature at which Kerr rotation became almost constant as shown in Fig. 3 (a) and (b). With increasing t_{Pd}, the T_C of the CoPd / Pd ML decreased and it became 110 ˚C at t_{Pd} = 5 nm, which is almost the same as that of the single stack of CoPd / Pd ML. Figure 4 (b) shows the difference between the Kerr rotation at a temperature of 170°C and that at room temperature for the 2nd cycle: cooling at H_{ext} = +40 Oe. The positive Kerr rotation indicates the switching of low T_C ML was determined by the H_{ext} direction, and the negative means the magnetization of low T_C ML became downward against the H_{ext} and the switching was controlled by the magnetization of the high T_C Co / Pd ML through the exchange coupling between CoPd / Pd and Co / Pd MLs. When $t_{Pd} \leq 1$ nm, the CoPd / Pd ML is reversed due to the exchange coupling, however when $t_{Pd} \geq 2$ nm the thermomagnetic writing dominated. For the efficient STT switching by using the T_CC hybrid structure, t_{Pd} was found to be limited to $t_{Pd} < 2$ nm.

FIGURE 4 HERE

C. *Tri-layer structure*

As a T_CC structure expected to be more efficient than the bi-layer stack, we fabricated tri-MLs stack as substrate / Ta (10 nm) / Pt (5 nm) / [Pt (1.2 nm) / Co (0.4 nm)]$_6$ ML / [Pd (1.2 nm) / $Co_{48}Pd_{52}$ (0.3 nm)]$_3$ ML / [Pd (1.2 nm) / Co (0.4 nm)]$_3$ ML / SiN (5 nm). The intermediate CoPd / Pd ML exhibits low T_C of ~110˚C, and we also fabricated the sample replacing the low T_C CoPd / Pd by Pd (4.5 nm) as a control sample. We refer to the former stack as stack A and the latter stack B.

Figure 5 (a) shows polar Kerr hysteresis loops of stack A at room temperature. The loop exhibits simple square shape indicating that the magnetizations of tri-MLs switch simultaneously due to the exchange coupling through the intermediate CoPd / Pd ML. On the other hand, at 172˚C, the loop exhibited two-step feature suggesting the Co / Pd and Co / Pt MLs switch independently as shown in Fig. 5 (b). The H_c of the two MLs were similar to those of stack B with an intermediate Pd 4.5 nm as shown in Fig. 5 (d). Figures 5 (c) and (d) show the Kerr loops of the stack B measured at room temperature and 132˚C, respectively. For the stack B, the two-steps features were obvious even at room temperature.

FIGURE 5 HERE

Figures 6 (a) and (b) show temperature dependence of (a) Kerr rotation and (b) coercivities of the Co / Pd and Co / Pt MLs estimated from the hysteresis loops shown in Figs. 5 (a) and (b). The Kerr rotation gradually decreased with increasing the temperature. The coercivities of the two layers were identical up to 120 ˚C, indicating the two MLs switch simultaneously, and then the two-step feature with different H_c of Co / Pd and Co / Pt MLs was obvious above 130˚C. This temperature is roughly consistent with T_C of the intermediate CoPd / Pd ML. The H_c of Co / Pd (Co / Pt) ML decreased (increased) with increasing the temperature, which may indicate the gradual decrease of the exchange coupling through the CoPd / Pd ML by elevating the temperature. In order to realize the efficient STT switching using tri-layers structure, the exchange coupling between the two high T_C layers was considered to be controlled by the intermediate low T_C layer. In the tri-MLs structure with high T_C Co / Pt and Co / Pd MLs and low T_C CoPd / Pd ML, these coupled and decoupled situations were found to be realized by changing the temperature from room temperature to around 150˚C. The decoupling between the high T_C layers is considered to effectively reduce the critical current in the STT switching.

FIGURE 6 HERE

IV. CONCLUSION

In this study we designed two kinds of T_CC hybrid stacks to achieve high-density STT-MRAM. One is the high T_C / low T_C bi-layered hybrid stack which is expected to have significant gain (~4) of the ratio Δ / I_c compared to the conventional single layer. The other hybrid structure is a tri-layered stack with high T_C / low T_C / high T_C layers, which is expected to be more efficient than bi-layers stack.

First, we confirmed the magnetic properties of Co / Pd and CoPd / Pd MLs as the high and low T_C layers, respectively. Co / Pd ML was confirmed to exhibit a large perpendicular anisotropy and T_C much higher than 200˚C. Moreover, CoPd / Pd ML was confirmed to have low T_C of 110 ˚C without sacrificing the large perpendicular anisotropy.

Next, we fabricated bi-layered hybrid structure as [Co / Pd] ML / Pd (t_{Pd}) / [CoPd / Pd] ML with various intermediate Pd layer thicknesses to control the exchange coupling between the MLs. For $t_{Pd} \leq 1$ nm, the Co / Pd and CoPd / Pd MLs were confirmed to be exchange-coupled at room temperature. The increase of t_{Pd} reduced the strength of the exchange coupling, and we concluded that t_{Pd} should be less than 2 nm to be used in the T_CC hybrid stack. From the temperature dependence of the Kerr rotation of the bi-layered stack, the magnetization of the low T_C CoPd / Pd ML was confirmed to disappear around 110˚C, and the magnetization direction of the CoPd / Pd ML was switched following the magnetization of the high T_C Co / Pd ML at high temperature (~170˚C).

Finally, the tri-layered structure with a stack of [Co / Pt] ML / [CoPd / Pd] ML / [Co / Pd] ML was investigated as a T_CC memory layer to achieve further efficient switching. The tri-MLs stack showed one-step hysteresis loop at room temperature and two-steps loop at higher than 120˚C due to the loss of magnetic order of the intermediate low T_C CoPd / Pd ML. This means the exchange coupling between the two high T_C layers were controlled by the intermediate low T_C layer at relatively small temperature change from room temperature to ~150˚C.

Acknowledgment

The authors thank Mr. M. Kumazawa of Nagoya University for his assistance with the experiments. The authors are grateful for financial support by JSPS KAKENHI Grant Number 16H04328, 16K18091, 17H03249, 17K18878. A part of this work was conducted at the Nagoya University Nanofabrication Platform, supported by "Nanotechnology Platform Program" of the Ministry of Education, Culture, Sports, Science and Technology (MEXT), Japan.

References

[1] J. C. Slonczewski, “Current-driven excitation of magnetic multilayers,” *J. Magn. Magn. Mater.*, vol. 159, no. 1–2, pp. L1–L7, 1996.

[2] L. Berger, “Emission of spin waves by a magnetic mulitlayer traversed by a current,” *Phys. Rev. B*, vol. 54, no. 13, pp. 9353–9358, 1996.

[3] Z. Diao *et al.*, “Spin-transfer torque switching in magnetic tunnel junctions and spin-transfer torque random access memory,” *J. Phys. Condens. Matter*, vol. 19, p. 165209, 2007.

[4] I. L. Prejbeanu, M. Kerekes, R. C. Sousa, H. Sibuet, B. Dieny, and J. P. Nozières, “Thermally assisted MRAM,” *J. Phys. Condens. MATTER*, vol. 19, p. 165218, 2007.

[5] I. L. Prejbeanu, S. Bandiera, J. Alvarez-Hérault, R. C. Sousa, B. Dieny, and J. P. Nozières, “Thermally assisted MRAMs: Ultimate scalability and logic functionalities,” *J. Phys. D. Appl. Phys.*, vol. 46, no. 7, p. 74002, 2013.

[6] B. Dai, T. Kato, S. Iwata, and S. Tsunashima, “Spin transfer torque switching of amorphous gdfeco with perpendicular magnetic anisotropy for thermally assisted magnetic memories,” *IEEE Trans. Magn.*, vol. 48, no. 11, pp. 3223–3226, 2012.

[7] B. Dai, T. Kato, S. Iwata, and S. Tsunashima, “Temperature dependence of critical current density of spin transfer torque switching amorphous GdFeCo for thermally assisted MRAM,” *IEEE Trans. Magn.*, vol. 49, no. 7, pp. 4359–4362, 2013.

[8] T. Higashide, B. Dai, T. Kato, D. Oshima, and S. Iwata, “Magnetodynamics Effective Damping Constant and Current Induced Magnetization Switching of GdFeCo / TbFe Exchange-Coupled Bilayers,” *Ieee Magn. Lett.*, vol. 7, p. 3505605, 2016.

[9] B. Dai, Y. Guo, J. Zhu, T. Kato, and S. Iwata, “Spin transfer torque switching in exchange- coupled amorphous GdFeCo / TbFe bilayers for thermally assisted MRAM application,” *J. Phys. D. Appl. Phys.*, vol. 50, p. 135005, 2017.

[10] R. J. Gambino and T. Suzuki, *Magneto-Optical Recording Materials 1st ed*. New York, IEEE Press, pp.33-42, 1999.

[11] S. Tsunashima, S. Masui, T. Kobayashi, and S. Uchiyama, “Magneto-optic Kerr effect of amorphous Gd-Fe-Co films,” *J. Appl. Phys.*, vol. 53, no. 11, pp. 8175–8177, 1982.

[12] S. Tsunashima, “Magneto-optical recording,” *J. Phys. D. Appl. Phys.*, vol. 34, pp. R87–R102, 2001.

[13] L. You, T. Kato, S. Tsunashima, and S. Iwata, “Dynamic heating in micron- and submicron-patterned TbFe films,” *Jpn. J. Appl. Phys.*, vol. 47, no. 1, pp. 146–149, 2008.

[14] L. You, T. Kato, S. Tsunashima, and S. Iwata, “Thermomagnetic writing on deep submicron-patterned TbFe films by nanosecond current pulse,” *J. Magn. Magn. Mater.*, vol. 321, no. 8, pp. 1015–1018, 2009.

[15] K. Machida, Y. Sonobe, and Y. Nakatani, “Numerical Study on a Novel Curie Temperature Controlled Hybrid Thermo-Magnetic Structure for Magnetic Random Access Memories,” *IEEE Trans. Magn.*, vol. 53, no. 11 , 2017.

[16] O. Muthsam, C. Vogler, and D. Suess, “Noise reduction in heat-assisted magnetic recording of bit-patterned media by optimizing a high/low Tc bilayer structure,” *J. Appl. Phys.*, vol. 122, no. 21, p. 213903, 2017.

[17] P. F. Carcia, A. D. Meinhaldt, and A. Suna, “Perpendicular magnetic anisotropy in Pd / Co thin film layered structures,” *J. Appl. Phys.*, vol. 47, no. 2, pp. 178–180, 1985.

[18] F. J. A. Den Broeder, H. C. Donkersloot, H. J. G. Draaisma, and W. J. M. De Jonge, “Magnetic properties and structure of Pd / Co and Pd/ Fe multilayers,” *J. Appl. Phys.*, vol. 61, p. 4317, 1987.

[19] W. B. Zeper, F. J. A. M. Greidanus, and P. F. Carcia, “Evaporated Co/Pt layered structures for magneto-optical recording,” *IEEE Trans. Magn.*, vol. 25, no. 5, pp. 3764–3766, 1989.

[20] F. W. Constant, “THE MAGNETIC PROPERTIES OF CERTAIN Pt—Co AND Pd—Co ALLOYS,” *Phys. Rev.*, vol. 36, pp. 1654–1660, 1930.

[21] K. Nakamura, S. Tsunashima, M. Hasegawa, and S. Uchiyama, “Perpendicular magnetic anisotropy of PdCo alloy in multilayered structure,” *J. Magn. Magn. Mater.*, vol. 93, pp. 462–464, 1991.

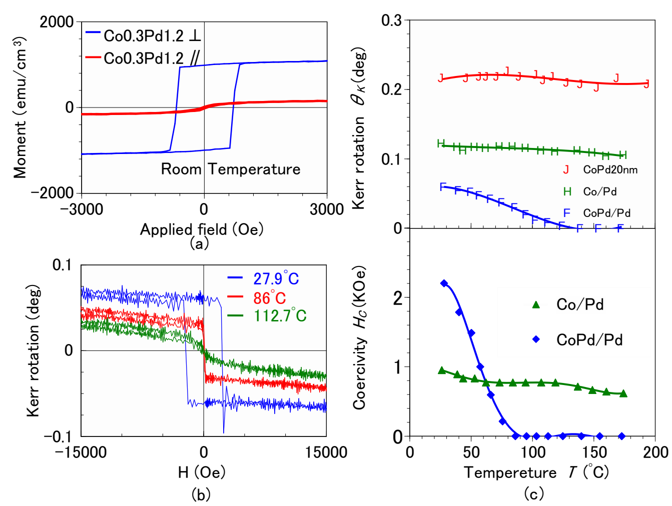

Fig. 1. (a) Perpendicular (blue) and in-plane (red) hysteresis loops of [Co (0.3 nm) / Pd (1.2 nm)]$_6$, (b) polar Kerr loops of [$Co_{54}Pd_{46}$ (0.3 nm) / Pd (1.2 nm)]$_6$ ML at different temperatures, and (c) temperature dependence of Kerr rotation and coercivities of CoPd alloy, Co / Pd ML and CoPd / Pd ML.

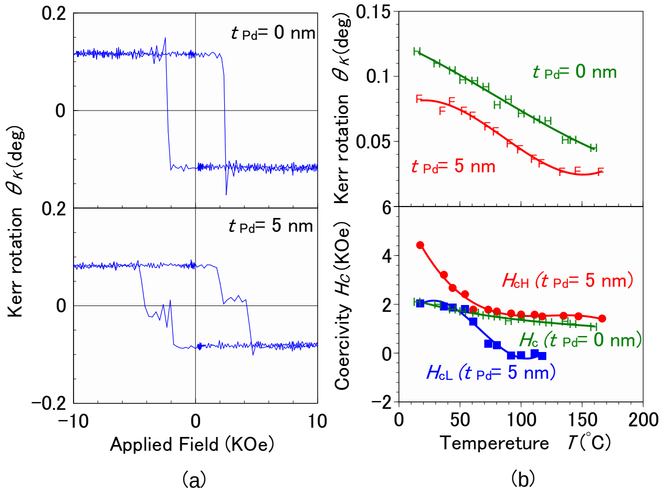

Fig. 2. (a) Polar Kerr loops of [CoPd (0.3 nm) / Pd (1.2 nm)]$_6$ / Pd (t_{Pd}) / [Co (0.3 nm) / Pd (1.2 nm)]$_6$ with t_{Pd} = 0 and 5nm, and (b) temperature dependences of Kerr rotation and coercivities of the stack with t_{Pd} = 0 and 5nm.

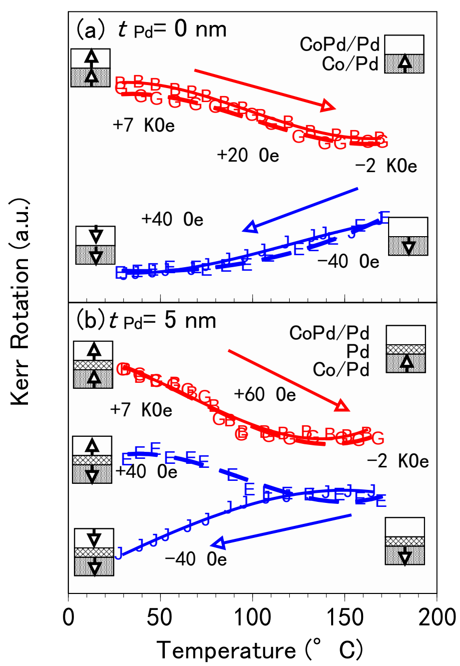

Fig. 3. Magnetization switching behavior of [CoPd (0.3 nm) / Pd (1.2 nm)]$_6$ / Pd (t_{Pd}) / [Co (0.3 nm) / Pd (1.2 nm)]$_6$ with t_{Pd} = (a) 0 nm and (b) 5 nm. Solid symbols are the result of the 1st cycle cooling under H_{ext} = –40 Oe and open symbols are for the 2nd cycle cooling under H_{ext} = +40 Oe.

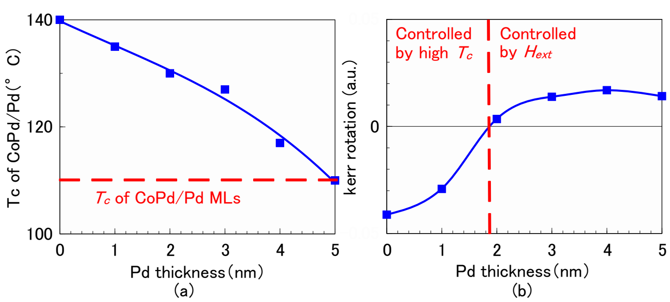

Fig. 4. (a) T_C of CoPd / Pd ML and (b) difference between the Kerr rotations at 170°C and after cooling under H_{ext} = +40 Oe for [CoPd (0.3 nm) / Pd (1.2 nm)]$_6$ / Pd (t_{Pd}) / [Co (0.3 nm) / Pd (1.2 nm)]$_6$.

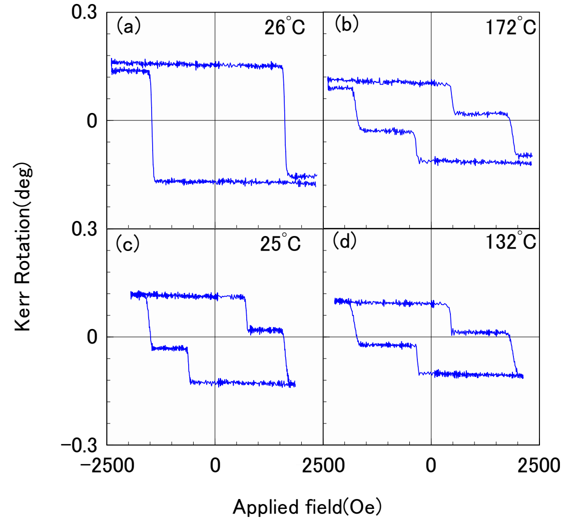

Fig. 5. Polar Kerr loops of stack A, [Co / Pt] / [CoPd / Pd] / [Co / Pd], measured at (a) 26°C and (b) 172°C and of stack B, [Co / Pt] / Pd / [Co / Pd], measured at (c) 25°C and (d) 132°C.

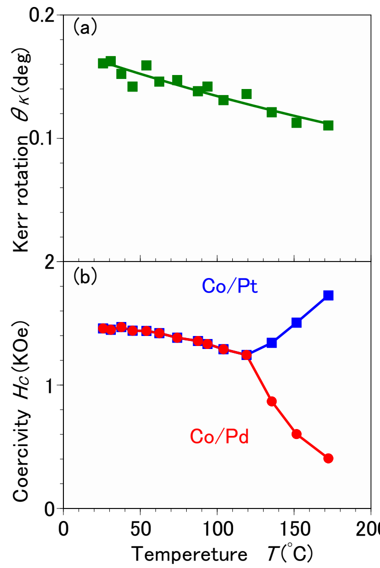

Fig. 6. Temperature dependences of (a) Kerr rotation and (b) coercivities of the stack A, [Co / Pt] / [CoPd / Pd] / [Co / Pd].